Presented at the 29th European PV Solar Energy Conference and Exhibition, 22-26 September 2014, Amsterdam, The Netherlands

RECOMBINATION CHARACTERISTICS OF P$^+$ REGIONS ALLOYED FROM SCREEN-PRINTED ALUMINUM PASTES CONTAINING BORON ADDITIVES

Michael Rauer, Heiko Steinkemper, Christian Schmiga, Markus Glatthaar and Stefan W. Glunz

Fraunhofer Institute for Solar Energy Systems (ISE)
Heidenhofstraße 2, 79110 Freiburg, Germany
Phone: +49(0)761/4588-5921, Fax: +49(0)761/4588-9250,
E-mail: michael.rauer@ise.fraunhofer.de

ABSTRACT: We present a detailed analysis of the recombination characteristics of p^+ regions alloyed into silicon from screen-printed aluminum pastes containing boron additives (Al-B pastes). By numerically simulating the saturation current densities corresponding to (i) recombination at the surfaces of the Al-B-codoped p^+ Si (Al-B-p^+) regions as well as (ii) Auger and (iii) defect recombination within their bulks, we show that the recombination characteristics are versatilely affected by the B additive within the paste: An increase in the effective B percentage, which is the percentage of B additive actually utilized, leads to a significant reduction of surface recombination and of defect recombination, but also to the simultaneous intensification of Auger recombination. The optimal effective B percentage, which has been calculated to 0.03 wt%, constitutes a compromise between these recombination mechanisms. By measuring the saturation current densities $j_{0,p+}$ of Al-B-p^+ regions, the optimal effective B percentage of 0.03 wt% has been verified experimentally. Excellently low $j_{0,p+}$ values of less than 260 fA/cm^2 have been achieved, corresponding to implied open-circuit voltages of more than 664 mV. Our simulations show that Al-B pastes of optimal composition provide a high robustness against variations of the alloying conditions, since their Al-B-p^+ saturation current densities are largely independent of the printed paste amount and the firing conditions. This allows for a more flexible fabrication of the front and rear contacts of Si solar cells during a single co-firing process.
Keywords: Aluminum-boron Codoping, Aluminum-boron Paste, Coalloying, Silicon Solar Cells

1 INTRODUCTION

Although screen-printed aluminum pastes containing boron additives (referred to as Al-B pastes) have been applied for the fabrication of the rear contacts of silicon solar cells for several years now [1], only few studies addressing the properties, particularly the formation and the recombination characteristics of Al-B-codoped p^+ Si (Al-B-p^+) regions have been published so far [2-4].

We have recently presented an analytical model for the formation of Al-B acceptor profiles by quantitatively describing (i) the composition of the Al-B-Si melt and (ii) the incorporation of Al and B acceptor atoms into the recrystallizing Si during alloying. We have demonstrated that measured Al-B acceptor profiles can be accurately described by this model [5, 6]. The additional incorporation of B atoms as acceptors into the p^+ region enhances the acceptor concentration within the p^+ region due to the high solid solubility of B in Si. Thus, the shielding of electrons from the recombination-active surface improves.

In this study, our analytical model is applied to investigate the electrical properties of Al-B-p^+ regions in more detail considering data of experiments and simulations. This allows for a deeper understanding of the recombination characteristics, enabling a further and straightforward optimization of the Al-B paste composition.

2 EXPERIMENTAL

To investigate the recombination characteristics of Al-B-p^+ regions experimentally, simple test samples were fabricated [5]. A silicon nitride layer (refractive index of 2.1) was deposited onto the front side of planar float-zone Si wafers by means of plasma-enhanced chemical vapor deposition. The composition of an Al base paste was systematically modified by adding elemental B powder to the paste, thus varying the B percentage f_B in the paste in the range from 0 to 0.9 wt%. Each paste was then screen-printed onto the rear surface of the samples (wet paste amount m_{paste} = 17.2 mg/cm^2). The Al-B-p^+ regions were alloyed in a conveyor belt furnace at a set peak temperature of 900 °C. By applying different peak temperature times, the *effective* peak temperature $T_{peak,eff}$, which is lower than the set peak temperature of the furnace due to the latent heat of the pastes and which was determined by phase diagram calculations [7], was varied from 650 °C to 860 °C. The eutectic layers and the paste residuals were finally removed in hydrochloric acid for the further electrical characterization.

We have measured the Al-B acceptor profiles via the electrochemical capacitance-voltage (ECV) technique, thereby correcting the profiles for the roughnesses of the p^+ region surfaces [3, 8]. We have additionally carried out quasi-steady state photoconductance (QSS-PC) measurements to determine the saturation current densities of the p^+ regions.

3 ANALYTICAL MODEL FOR ALLOYING FROM ALUMINUM PASTES CONTAINING BORON ADDITIVES

Figure 1 shows an ECV-measured Al-B acceptor profile of a p^+ region alloyed from an Al-B paste with f_B = 0.9 wt% at $T_{peak,eff}$ = 835 °C. The profile was recalculated analytically applying our above-mentioned model. The model thereby covers three essential characteristics of alloying from screen-printed Al-B pastes: (i) the recrystallization of Si within the paste particles, which reduces the growth of the p^+ region at the Si wafer surface for high paste amounts [7, 9, 10], (ii) the latent heat of the paste by applying effective peak temperatures [5, 7] and (iii) the incomplete dissolution of the boron additive [6, 11], which leads to a significant reduction of the *effective* B percentage $f_{B,eff}$.

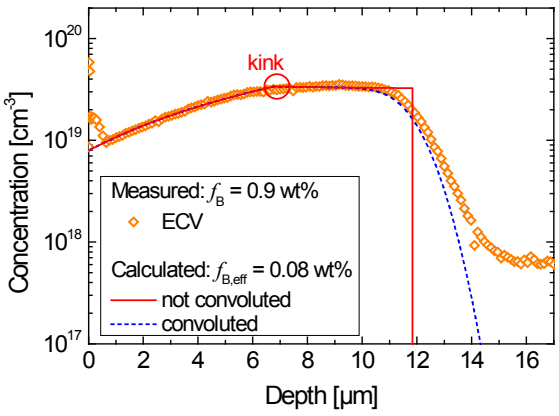

Figure 1: ECV-measured Al-B acceptor profile (orange symbols) of a p^+ region alloyed from an Al paste containing 0.9 wt% of elemental B. The profile was recalculated analytically (red line) assuming a reduced effective B percentage $f_{B,eff}$ = 0.08 wt%. The maximal depth of the calculated profile is thereby defined by $T_{peak,eff}$ = 835 °C. Because $f_{B,eff}$ could not be determined directly due to the incomplete dissolution of the B additive, $f_{B,eff}$ was taken as sole fit parameter for the calculation. To account for the blurring of the Al-p^+/Si base transition, which is a measurement artifact of the ECV technique, the calculated abrupt profile for $f_{B,eff}$ = 0.08 wt% has been convoluted with a Gaussian thickness distribution, resulting in the profile curve shown by the dashed blue line.

To recalculate the measured profile, an effective B percentage $f_{B,eff}$ = 0.08 wt% was used (see Figure 1), with $f_{B,eff}$ being the only free parameter of the calculation. Excellent accordance with the measured profile was achieved. In particular, the model accurately describes the formation of the characteristic kink in the acceptor profile curve to be caused by the maximal dissolution of the B additive during alloying [5, 6]. For an improved comparison of the calculated and the measured profiles, the blurring of the Al-p^+/Si base transition, which occurs as a measurement artifact of the ECV technique, has been included in the calculations by convoluting the calculated profile with a Gaussian thickness distribution [3, 8, 12]. The dashed blue line in Figure 1 shows the convoluted Al-B acceptor profile, which reproduces the ECV-measured curve very well. Our analytical model for alloying from Al-B pastes therefore provides a firm basis for calculating the recombination characteristics of Al-B-p^+ regions.

4 SIMULATION OF THE RECOMBINATION CHARACTERISTICS OF ALUMINUM-BORON-CODOPED P$^+$ REGIONS

Since the recombination characteristics of Al-B-p^+ regions are very complex, we carried out numerical simulations of Al-B-p^+ saturation current densities $j_{0,p+}$ using a recently published method [12] implemented in Sentaurus TCAD [13]. To accurately calculate $j_{0,p+}$, two effects were taken into account: (i) recombination via defects within the p^+ region bulks [12, 14, 15] and (ii) incomplete ionization of Al acceptors [3, 8, 12]. For B acceptors, incomplete ionization is significantly less pronounced [3, 16] and has therefore been neglected.

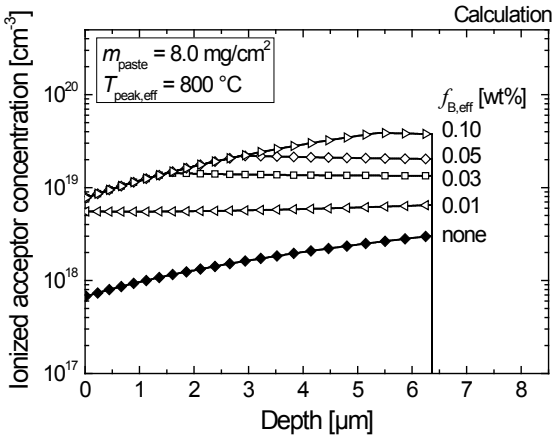

Figure 2: Calculated ionized Al-B acceptor profiles of p^+ regions formed by alloying from Al pastes containing $f_{B,eff}$ in the range of 0 to 0.1 wt% for m_{paste} = 8.0 mg/cm^2 and $T_{peak,eff}$ = 800 °C. Because both Al and B atoms contribute to the ionized acceptor concentration, the profiles are defined by the sum of the ionized Al and B acceptor atoms. Thereby, incomplete ionization of Al acceptors is particularly taken into account.

For the simulations, we applied acceptor profiles as input data. The profiles of ionized Al and B acceptors were therefore determined in dependence of (i) the printed paste amount m_{paste}, (ii) the effective peak temperature $T_{peak,eff}$ of the alloying process and (iii) the effective B percentage $f_{B,eff}$ in the paste, using our analytical model. Figure 2 shows the calculated ionized acceptor profiles of Al-B-p^+ regions formed by alloying from Al pastes containing different $f_{B,eff}$ values exemplarily for m_{paste} = 8.0 mg/cm^2 and $T_{peak,eff}$ = 800 °C. It is obvious that the peak concentrations of the acceptor profile curves increase with increasing $f_{B,eff}$ values, since more B atoms are incorporated into the p^+ regions as acceptors.

To analyze the recombination characteristics of Al-B-coalloyed p^+ regions in more detail, the saturation current densities corresponding to (i) recombination at their surface as well as (ii) Auger and (iii) defect recombination within their bulks were determined separately. Thus, a differentiated investigation of the entire Al-B-p^+ recombination characteristics is presented for the first time.

The effective B percentage $f_{B,eff}$ strongly affects the recombination characteristics of Al-B-codoped p^+ regions as shown in Figure 3 for m_{paste} = 8.0 mg/cm^2 and $T_{peak,eff}$ = 800 °C.

For $f_{B,eff} \lesssim 0.01$ wt%, surface recombination dominates the recombination characteristics. Auger recombination and defect recombination make only minor contributions. When the effective B percentage $f_{B,eff}$ is increased, the Al-B acceptor concentration increases. Thus, surface recombination is reduced significantly, since the diffusion of electrons toward the surface of the p^+ region is slowed down [17]. Simultaneously, Auger recombination, which depends on the square of the acceptor concentration [18, 19], intensifies and becomes the dominant recombination mechanism for $f_{B,eff} \gtrsim 0.05$ wt%. Although the density of defects within the p^+ regions is assumed to be independent of $f_{B,eff}$ [5, 11], the defect recombination decreases due to the increasing Auger recombination.

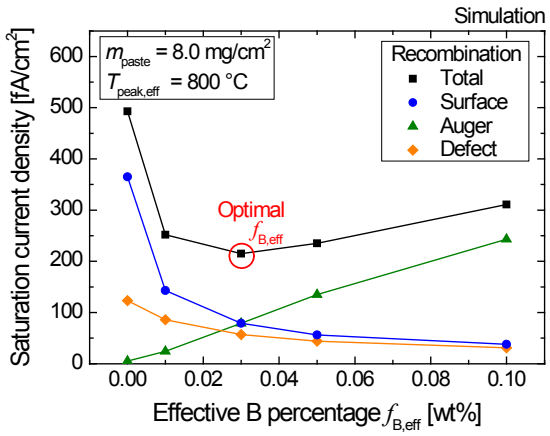

Figure 3: Calculated saturation current densities for the Al-B acceptor profiles presented in Figure 2. In addition to the total saturation current densities (black squares), the separate contributions originating from recombination at the p^+ region surfaces (blue circles) as well as Auger (green triangles) and defect recombination (orange diamonds) within the p^+ region bulks were calculated. The total saturation current density exhibits a distinct minimum for $f_{B,eff} \approx 0.03$ wt%.

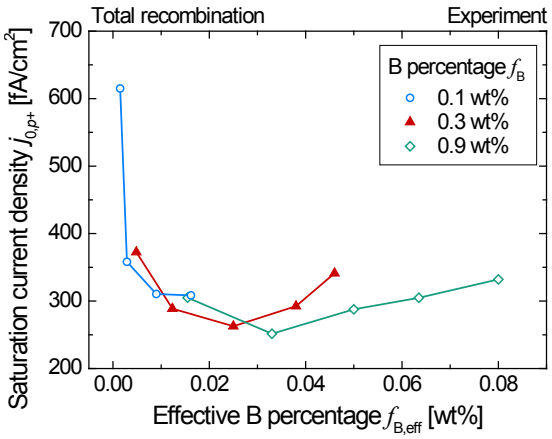

Figure 4: Measured total saturation current densities $j_{0,p+}$ as a function of the effective B percentage $f_{B,eff}$ for different percentages f_B of elemental B as additive within the paste. An intrinsic carrier concentration $n_i = 9.65 \cdot 10^9$ cm^{-3} [20] has been used.

The total recombination current density, which is the sum of the surface, Auger and defect saturation current densities, therefore exhibits a minimum at $f_{B,eff} = 0.03$ wt%, which is a compromise between the three recombination mechanisms.

5 EXPERIMENTAL EVALUATION OF THE RECOMBINATION CHARACTERISTICS

Figure 4 shows the measured total saturation current densities $j_{0,p+}$ of various Al-B-p^+ regions as a function of their $f_{B,eff}$ values, which were determined by recalculating the measured Al-B profiles [6]. It is evident that the $j_{0,p+}$ values decrease for increasing $f_{B,eff}$ values and exhibit a broad minimum at an effective B percentage of approximately 0.03 wt%. Thus, the experimental $j_{0,p+}$ values are in excellent agreement with the trends of our numerical simulations presented above.

The experimental realization of the optimal effective B percentage is not straightforward for elemental B powder as additive within the paste, though. Since the utilization of the elemental B additive strongly depends on the firing conditions [6] due to its slow dissolution behavior, the optimal $f_{B,eff}$ value of 0.03 wt% is realized at different $T_{peak,eff}$ values for the different percentages f_B of elemental B [5]: The higher f_B, the lower the effective peak temperature of the $j_{0,p+}$ minimum. Thus, in practice, there is no specific optimum for the printing and firing conditions. Instead, the effective peak temperature needs to be adapted carefully to the B percentage f_B in the paste, so as to adjust the *effective* B percentage $f_{B,eff}$ to 0.03 wt%.

Remarkably low saturation current densities of less than 260 fA/cm^2 have been achieved experimentally for $f_B = 0.3$ and 0.9 wt% at $T_{peak,eff} = 795$ and 767 °C, respectively, corresponding to implied open-circuit voltages of more than 664 mV.

6 POTENTIAL OF ALUMINUM-BORON PASTES OF OPTIMIZED COMPOSITION

In order to assess the potential of Al-B pastes of optimal composition, the total saturation current density $j_{0,p+}$ was simulated as a function of the effective peak temperature for different paste amounts from 4.5 to 25 mg/cm^2 and the optimal effective B percentage of 0.03 wt%, see Figure 5. It is clearly visible that for $m_{paste} \gtrsim 8$ mg/cm^2 and $T_{peak,eff} \gtrsim 750$ °C, the $j_{0,p+}$ values are nearly independent of m_{paste} and $T_{peak,eff}$ and on an excellently low level, below 250 fA/cm^2. Thus, Al-B pastes of optimal composition provide excellent recombination characteristics and a high robustness and stability against variations of m_{paste} and $T_{peak,eff}$.

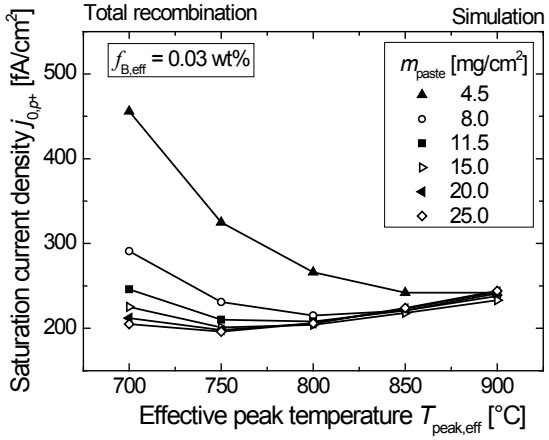

Figure 5: Calculated total saturation current densities $j_{0,p+}$ of Al-B-p^+ regions as a function of the effective peak temperature $T_{peak,eff}$ for the optimal effective B percentage $f_{B,eff} = 0.03$ wt%. Paste amounts in the range from 4.5 to 25 mg/cm^2 were used for the simulations. For $m_{paste} \gtrsim 8$ mg/cm^2 and $T_{peak,eff} \gtrsim 750$ °C, the saturation current densities are nearly independent of m_{paste} and $T_{peak,eff}$, thus enabling a very flexible application of these Al-B pastes.

Since the incomplete dissolution of the elemental B additive complicates the experimental realization of the optimized paste composition, further paste optimization will deal with investigating B additives that dissolve instantaneously during alloying.

7 SUMMARY

In this paper, we have investigated the recombination characteristics of p^+ regions formed by alloying from screen-printed Al pastes containing B additives by means of experiments and simulations.

Our numerical simulations have shown that an increase in the effective B percentage in the paste leads to a significant reduction of surface recombination and of recombination at defects within the p^+ region bulks, but also to the simultaneous intensification of Auger recombination within the p^+ region bulks. The optimal effective B percentage, which has been calculated to 0.03 wt%, thus is a compromise between these recombination mechanisms.

We have confirmed the optimal effective B percentage experimentally and achieved excellently low saturation current densities of less than 260 fA/cm^2 ($n_i = 9.65 \cdot 10^9$ cm^{-3}). This corresponds to implied open-circuit voltages of more than 664 mV. The experiments have also shown that the incomplete dissolution of the B additive, which depends strongly on the firing conditions of the alloying process, complicates the realization of the optimal effective B percentage. In practice, the paste composition and the firing conditions need to be adapted to each other carefully.

We have pointed out the remarkable potential of Al pastes containing B with optimal percentage. Our simulations have demonstrated that saturation current densities of Al-B-p^+ regions alloyed from these pastes are on an excellently low level and largely independent of the paste amount and the firing conditions. Thus, Al-B pastes of optimized composition provide excellent recombination characteristics and an improved robustness against variations in the printing and firing conditions.

ACKNOWLEDGEMENTS

The authors would like to thank all colleagues of Fraunhofer ISE cleanroom and PV-TEC team and all other members of SEC department for their contributions to this work. Michael Rauer wants to thank the Reiner Lemoine Stiftung for funding.

REFERENCES

[1] Glunz, S.W. *High-efficiciency silicon solar cells – Research and production*. Presented at the *27th European Photovoltaic Solar Energy Conference and Exhibition*. 2012. Frankfurt, Germany.

[2] Lölgen, P., et al., *Boron doping of silicon using coalloying with aluminium.* Applied Physics Letters, 1994. **65**(22): p. 2792-4.

[3] Huster, F. and G. Schubert. *ECV doping profile measurements of aluminium alloyed back surface fields*. in *Proceedings of the 20th European Photovoltaic Solar Energy Conference*. 2005. Barcelona, Spain.

[4] Gu, X., X. Yu, and D. Yang, *Efficiency improvement of crystalline silicon solar cells with a back-surface field produced by boron and aluminum co-doping.* Scripta Materialia, 2012. **66**: p. 394–397.

[5] Rauer, M., et al. *Investigation of Aluminum-boron Doping Profiles Formed by Coalloying from Screen-printed Pastes*. in *Proc. 4th Metallization Workshop, Energy Procedia*. 2013. Constance, Germany: Energy Procedia.

[6] Rauer, M., et al., *Theoretical and experimental investigation of aluminum-boron codoping of silicon.* in preparation for submission, 2014.

[7] Rauer, M., et al., *Quantitative theoretical and experimental analysis of alloying from screen-printed aluminum paste on silicon.* in preparation for submission, 2014.

[8] Rauer, M., et al., *Incomplete ionization of aluminum in silicon and its effect on accurate determination of doping profiles.* J. Appl. Phys., 2013. **114**(21).

[9] Huster, F. *Investigation of the alloying process of screen printed aluminium pastes for the BSF formation on silicon solar cells*. in *Proceedings of the 20th European Photovoltaic Solar Energy Conference*. 2005. Barcelona, Spain.

[10] Krause, J., et al., *Microstructural and electrical properties of different-sized aluminum-alloyed contacts and their layer system on silicon surfaces.* Solar Energy Materials and Solar Cells, 2011. **95**(8): p. 2151-60.

[11] Rauer, M., et al., *Alloying from screen-printed aluminum pastes containing boron additives.* IEEE Journal of Photovoltaics, 2013. **3**(1): p. 206-11.

[12] Rüdiger, M., et al., *Effect of incomplete ionization for the description of highly aluminum-doped silicon.* Journal of Applied Physics, 2011. **110**: p. 024508.

[13] Sentaurus TCAD, *release D-2010.03*. 2010, Synopsys: Zürich, Switzerland.

[14] Schmidt, J., et al., *Recombination lifetimes in highly aluminum-doped silicon.* Journal of Applied Physics, 2009. **106**(9): p. 093707.

[15] Altermatt, P.P., et al. *Highly predictive modelling of entire Si solar cells for industrial applications*. in *Proceedings of the 24th European Photovoltaic Solar Energy Conference*. 2009. Hamburg, Germany.

[16] Altermatt, P.P., et al., *A simulation model for the density of states and for incomplete ionization in crystalline silicon. II. Investigation of Si:As and Si:B and usage in device simulation.* Journal of Applied Physics, 2006. **100**(11): p. 113715.

[17] Cuevas, A. and D. Yan, *Misconceptions and Misnomers in Solar Cells.* IEEE Journal of Photovoltaics, 2013. **3**(2): p. 916-923.

[18] Kerr, M.J. and A. Cuevas, *General parameterization of Auger recombination in crystalline silicon.* Journal of Applied Physics, 2002. **91**(4): p. 2473-80.

[19] Richter, A., et al., *Improved quantitative description of Auger recombination in crystalline silicon.* Physical Review B, 2012. **86**(16): p. 165202.

[20] Altermatt, P.P., et al., *Reassessment of the intrinsic carrier density in crystalline silicon in view of band-gap narrowing.* Journal of Applied Physics, 2003. **93**(3): p. 1598-604.